Anal. Chem. **2003,** *75,* 3837−3844

Mono- and Multilayer Formation by Diazonium Reduction on Carbon Surfaces Monitored with Atomic Force Microscopy "Scratching"

Franklin Anariba, Stacy H. DuVall, and Richard L. McCreery*

Department of Chemistry, The Ohio State University, Columbus, Ohio 43210

Contact mode atomic force microscopy (AFM) was used to intentionally scratch a monolayer deposited on a pyrolyzed photoresist film (PPF). The force was set to completely remove the monolayer but not to damage the underlying PPF surface. A line profile determined across the scratch with tapping mode AFM permitted determination of the monolayer thickness from the depth of the scratch. A statistical process was devised to avoid user bias in determining the monolayer thickness and was used to determine the thickness as a function of derivatization parameters. PPF surfaces modified by reduction of diazonium ions of stilbene, biphenyl, nitrobiphenyl, terphenyl, and nitroazobenzene (NAB) were scratched and their modification layer thicknesses determined. For single-scan derivatizations of 1 mM diazonium ions to −0.6 V versus Ag^+/Ag, the biphenyl and stilbene monolayers exhibited thicknesses close to those expected for true monolayers. However, more extensive derivatization resulted in multilayers up to 6.3 nm thick for the case of NAB. Such multilayers imply that electrons are transmitted through the growing film during diazonium reduction, despite the fact that electron tunneling would not be expected to be operative over such long distances. The results are consistent with a conductance increase in the growing film, which yields a partially conductive layer that can support further diazonium ion reduction and additional layer growth.

Covalent bonding of a variety of molecules to carbon electrode surfaces via phenyldiazonium ion reduction is a relatively recent addition to the arsenal of methods for modifying electrode surfaces.[1−11] Electrochemical reduction of diazonium ion reagents in water or acetonitrile produces free N_2 and a reactive phenyl radical, which irreversibly binds to carbon surfaces, particularly glassy carbon and carbon fibers. The high reactivity of phenyl radicals produces densely packed monolayers on carbon, which often exhibit negligible observable pinholes. The strong, covalent C−C bond is stable, and a wide variety of diazonium reagents are either available commercially or via a one-step synthesis from an aromatic amine. Applications of carbon electrodes modified via diazonium reduction include electrode kinetic investigations,[12−15] adhesion promotion in carbon fiber composites,[2,16] and improvements in electroanalytical selectivity and electrocatalysis.[9,11,13,14] Examples of the electrochemical effects of diazonium modification include enhanced activity for dopamine oxidation with an anthraquinone monolayer,[14] minor inhibition of electron transfer to methyl viologen,[17] and complete inhibition of dopamine oxidation.[13,14] The structure of the diazonium reagent is easily varied by substitution of the phenyl ring, permitting a wide range of electrode surface behavior.

Although the strong bonding and dense packing of monolayers produced by diazonium reduction are well established, there is uncertainty about the modification layer thickness. Kariuki and McDermott used scanning probe microscopy to demonstrate that reduction of diethylaminophenyldiazonium ion can produce multilayers with thicknesses of ∼20 nm under certain conditions, particularly high diazonium ion concentration and long reduction times.[5] They also provided FT-IR evidence for the attack of the initial monolayer by a second layer of electrogenerated radical. A related paper demonstrated that diazonium reduction on highly ordered pyrolytic graphite nucleated at defects and then grew into multilayer "mushrooms" by continued radical generation.[4] Our laboratory has reported multilayers produced by nitroazobenzenediazonium ion reduction, with substantial effects on molecular junctions compared to those made from monolayers.[18,19] Since most applications of surface modification are critically dependent

* Corresponding author. E-mail: mccreery.2@osu.edu.

(1) Allongue, P.; Delamar, M.; Desbat, B.; Fagebaume, O.; Hitmi, R.; Pinson, J.; Saveant, J. M. *J. Am. Chem. Soc.* **1997**, *119*, 201.
(2) Delamar, M.; Desarmot, G.; Fagebaume, O.; Hitmi, R.; Pinson, J.; Saveant, J. *Carbon* **1997**, *35*, 801.
(3) Delamar, M.; Hitmi, R.; Pinson, J.; Saveant, J. M. *J. Am. Chem. Soc.* **1992**, *114*, 5883.
(4) Kariuki, J. K.; McDermott, M. T. *Langmuir* **1999**, *15*, 6534.
(5) Kariuki, J. K.; McDermott, M. T. *Langmuir* **2001**, *17*, 5947.
(6) Liu, Y.-C.; McCreery, R. L. *Anal. Chem.* **1997**, *69*, 2091.
(7) Liu, Y.-C.; McCreery, R. L. *J. Am. Chem. Soc.* **1995**, *117*, 11254.
(8) Itoh, T.; McCreery, R. L. *J. Am. Chem. Soc.* **2002**, *124*, 10894.
(9) Downard, A. J. *Electroanalysis* **2000**, *12*, 1085.
(10) Downard, A. J.; Roddick, A. D. *Electroanalysis* **1995**, *7*, 376.
(11) Downard, A. J. *Langmuir* **2000**, *16*, 9680.
(12) DuVall, S.; Yang, H.-H.; McCreery, R. L. *Control of Electron Transfer Kinetics of Organic Redox Systems on Carbon Electrodes*; 1999; Vol. 99.
(13) DuVall, S.; McCreery, R. L. *Anal. Chem.* **1999**, *71*, 4594.
(14) DuVall, S.; McCreery, R. L. *J. Am. Chem. Soc.* **2000**, *122*, 6759.
(15) Chen, P.; McCreery, R. L. *Anal. Chem.* **1996**, *68*, 3958.
(16) Coulon, E.; Pinson, J.; Bourzat, J.-D.; Commercon, A.; Pulicani, J.-P. *Langmuir* **2002**, *17*, 7102.
(17) Yang, H.-H.; McCreery, R. L. *Anal. Chem.* **1999**, *71*, 4081.
(18) Ranganathan, S.; Steidel, I.; Anariba, F.; McCreery, R. L. *Nano Lett.* **2001**, *1*, 491.
(19) Solak, A. O.; Ranganathan, S.; Itoh, T.; McCreery, R. L. *Electrochem. Solid State Lett.* **2002**, *5*, E43.

10.1021/ac034026v CCC: $25.00
Published on Web 06/20/2003

on layer thickness, it is usually essential to be aware of possible multilayer formation. On a more general note, multilayers on modified electrodes have been studied by a variety of techniques, including profilometry,[20,21] FT-IR,[22] ellipsometry,[21] and atomic force microscopy (AFM).[23,24] In some cases, an intentional "scratch" was made in the modification layer with an AFM tip in order to assess the layer thickness.[23−27]

The current experiments were directed toward three objectives bearing on the issue of multilayer formation from diazonium ion reduction. First, an AFM method was sought that yielded a direct measure of layer thickness. Second, the conditions that result in multilayer formation were determined for several diazonium reagents. Third, the perplexing question of how thick (>40 Å) multilayers can form by electrochemical reduction was addressed. Since electron tunneling should be very slow over such distances, it is not obvious how diazonium ion reduction can occur once a ∼40-Å layer is present. An AFM approach based on intentional "scratching" of the surface followed by noncontact AFM similar to that of Frankel et al.[25−27] and Bradley et al.[23] was exploited to address these questions about diazonium ion modification of carbon surfaces.

EXPERIMENTAL SECTION

The procedure for preparing pyrolyzed photoresist films (PPF) has been described previously.[28,29] Briefly, positive photoresist AZ P4330-RS (Clariant Corp., Sumerville, NJ) was spin-coated onto clean silicon at 6000 rpm on a spin coater (PWM101, Headway Research Inc., Garland, TX) for 30 s. Three coatings were applied, with a final film thickness of 5−6 μm. The spin-coated samples were then soft baked at 90 °C for 20 min, and pyrolysis took place in a tube furnace (Lindberg) fitted with a quartz tube. The tube was flushed by a continuous flow of forming gas (95% N_2 + 5% H_2) at ∼100 sccm during pyrolysis and cooling; samples were heated at 20 °C/min to 1000 °C, held at 1000 °C for 60 min, and then allowed to cool to room temperature while gas remained flowing.

Electrochemical experiments were performed with a BAS 100-W potentiostat (Bioanalytical Systems, West Lafayette, IN). An Ag^+/Ag (0.01 M) (Bioanalytical Systems) reference electrode calibrated to the $E_{1/2}$ of ferrocene was used for derivatization. An observed $E_{1/2}$ for Fc of 89 mV versus Ag^+/Ag established the Ag^+/Ag potential to be +0.22 V versus aqueous SCE, based on an Fc $E°$ of +0.31 V. versus aqueous SCE.[30] Contact to the PPF substrate was made with an alligator clip to the top surface of the PPF.

Derivatization of PPF surfaces was performed by the reduction of the corresponding diazonium salt in acetonitrile (Aldrich) with *n*-tetrabutylammonium tetrafluoroborate (0.1 M; Aldrich) as the supporting electrolyte. Tetrafluoroborate diazonium salts of 4-nitroazobenzene-4′- (NAB), stilbene (SB), biphenyl (BP), nitrobiphenyl (NBP), and terphenyl (TP) were prepared according to previously established procedures.[6,31] It was essential to ensure the diazonium salt solutions were freshly prepared, degassed thoroughly with argon, and had low water content before derivatization. The concentration of the diazonium salt solution was 1 mM, and derivatization scans were from +0.4 to −0.6 V versus Ag^+/Ag at 200 mV/s except where noted. After derivatization, PPF samples were immediately rinsed with 30 mL of acetonitrile and then kept in clean acetonitrile until ready for analysis. Unless noted otherwise, solvents were treated with activated carbon and filtered before use. Other reagents included isopropyl alcohol (Mallinckrodt Inc.) and activated carbon (Darco S-51, Norit Americas Inc.).

Atomic force microscopy measurements were carried out in air with a Nanoscope IIIa Multimode instrument (Digital Instruments, Santa Barbara, CA). Rotated tapping mode etched silicon probes (RTESP) with resonant frequencies of ∼300 kHz were purchased from Veeco (Sunnyvale, CA). The AFM tip was replaced after several "scratches," and its resonant frequency was checked frequently to test for tip damage or possible residue adhering to the tip. The *Z*-axis of the AFM was calibrated with a standard grid provided by Digital Instruments. The force used for scratching was determined empirically as described in the Results section but was ∼1 μN. Height measurements were made in tapping mode and scratches were made in contact mode. The images were acquired with a scan rate of either 0.5 or 1.0 Hz and were flattened with a first-order polynomial before analysis. The apparent "ripple" with a period of ∼0.2 μm is due to electronic or mechanical interference, and its period appearance depends on the scan rate. The inability to reproduce the position of the "ripples" on repetitive scans indicates they do not represent real variations in sample height. Filtering was adjusted on the AFM to reduce interference as much as possible without seriously degrading resolution.

Theoretical thicknesses for monolayers were calculated using Gaussian 98[32] with density functional theory (B3LYP/6-31G(d)). Thickness was defined as the length of the molecule bonded perpendicularly to the PPF surface, including the van der Waal radius of the terminal atom and a C−C single bond length between the surface and the phenyl ring carbon atom bonded to the surface.

(20) McCarley, R. L.; Morita, M.; Wilbourn, K. O.; Murray, R. W. *J. Electroanal. Chem.* **1988**, *245*, 321.
(21) McCarley, R. L.; Thomas, R. E.; Irene, E. A.; Murray, R. W. *J. Electrochem. Soc.* **1990**, *137*, 1485.
(22) McCarley, R. L.; Thomas, R. E.; Irene, E. A.; Murray, R. W. *J. Electroanal. Chem.* **1990**, *290*, 79.
(23) Ton-That, C.; Shard, A. G.; Bradley, R. H. *Langmuir* **2000**, *16*, 2281.
(24) Nishikawa, T.; Nishida, J.; Ookura, R.; Nishimura, S.-I.; Scheumann, V.; Zizlsperger, M.; Lawall, R.; Knoll, W.; Shimomura, M. *Langmuir* **2000**, *16*, 1337.
(25) Devecchio, D.; Schmutz, P.; Frankel, G. *Electrochem. Solid State Lett.* **2000**, *3*, 90.
(26) Schmutz, P.; Frankel, G. S. *J. Electrochem. Soc.* **1999**, *146*, 4461.
(27) Leblanc, P.; Frankel, G. *J. Electrochem Soc.* **2002**, *129*, B239.
(28) Ranganathan, S.; McCreery, R. L.; Majji, S. M.; Madou, M. *J. Electrochem. Soc.* **2000**, *147*, 277.
(29) Ranganathan, S.; McCreery, R. L. *Anal. Chem.* **2001**, *73*, 893.
(30) Bard, A. J.; Faulkner, L. R. *Electrochemical Methods*, 2nd ed.; Wiley: New York, 2001.
(31) Solak, A. O.; Eichorst, L. R.; Clark, W. J.; McCreery, R. L. *Anal. Chem.* **2003**, *75*, 296.
(32) Frisch, M. J.; Trucks, G. W.; Schlegel, H. B.; Scuseria, G. E.; Robb, M. A.; Cheeseman, J. R.; Zakrzewski, V. G.; Montgomery, J. J. A.; Stratmann, R. E.; Burant, J. C.; Dapprich, S.; Millam, J. M.; Daniels, A. D.; Kudin, K. N.; Strain, M. C.; Farkas, O.; Tomasi, J.; Barone, V.; Cossi, M.; Cammi, R.; Mennucci, B.; Pomelli, C.; Adamo, C.; Clifford, S.; Ochterski, J.; Petersson, G. A.; Ayala, P. Y.; Cui, Q.; Morokuma, K.; Malick, D. K.; Rabuck, A. D.; Raghavachari, K.; Foresman, J. B.; Cioslowski, J.; Ortiz, J. V.; Baboul, A. G.; Stefanov, B. B.; Liu, G.; Liashenko, A.; Piskorz, P.; Komaromi, I.; Gomperts, R.; Martin, R. L.; Fox, D. J.; Keith, T.; Al-Laham, M. A.; Peng, C. Y.; Nanayakkara, A.; Gonzalez, C.; Challacombe, M.; Gill, P. M. W.; Johnson, B.; Chen, W.; Wong, M. W.; Andres, J. L.; Gonzalez, C.; Head-Gordon, M.; Replogle, E. S.; Pople, J. A. Gaussian 98; A.7 ed.; Gaussian, Inc.: Pittsburgh, 1998.

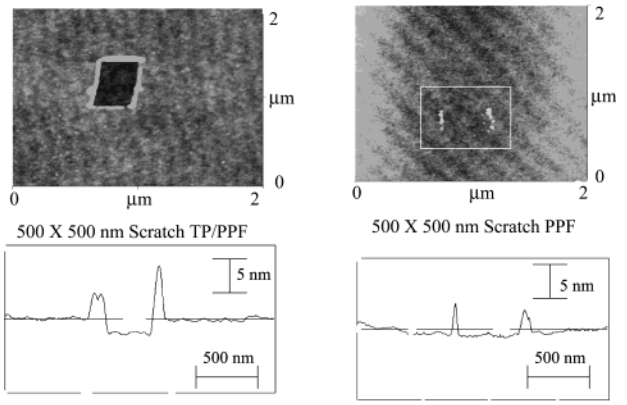

Figure 1. Upper left: tapping mode AFM image of a terphenyl monolayer showing a 500 × 500 nm trench in the monolayer formed with contact mode AFM. Lower left: line profile across the trench in upper image. Upper right: tapping mode image of bare PPF, with the white box framing a 500 × 500 nm scratch made in contact mode. Lower right: line profile through the image in the upper right.

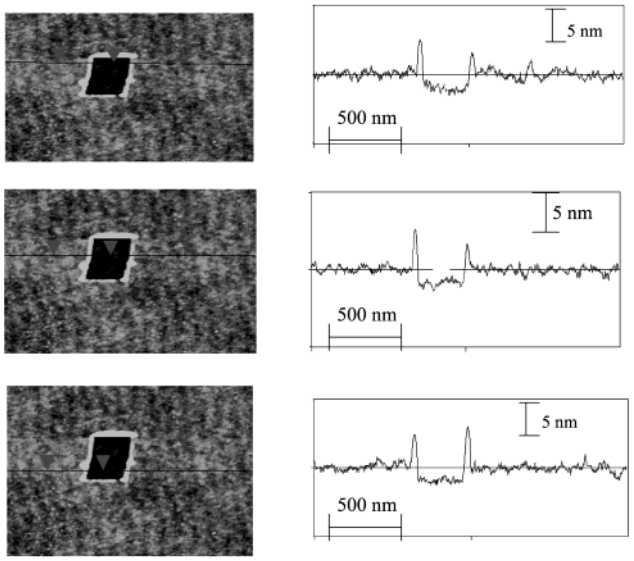

Figure 2. Three random single line profiles through a scratch in a terphenyl monolayer, along the lines shown in the images.

RESULTS

The term "AFM scratching" is used here to describe intentional damage to a modification layer on a relatively hard substrate.[23−27] If the applied force is sufficient to disrupt the monolayer but not to damage the substrate, it is possible to "carve out" a rectangular trench in the monolayer. The PPF substrate used here is similar to glassy carbon and is quite hard. A set-point voltage of 0.05 V in contact mode was initially used to scratch a stilbene monolayer. However, it was found that the depths of the trenches varied with scratch and scan area, an indication that the force being applied could be easily offset by tip−sample interactions. The set-point voltage was increased until trenches with flat bottoms and consistent depths were observed. The depth of the scratches did not change between set-point voltages of 0.20 and 0.25 V, and minimal variation in trench depth was observed at these voltages. A set-point voltage value of 0.25 V provided even-bottomed scratches with minimal variation in roughness (rms) inside and outside the scratch region. The independence of observed trench depth on set-point voltage implies that the monolayer was completely removed. However, a set-point voltage of 0.25 V proved too weak to scratch the unmodified PPF surface. As a consequence, a set-point voltage force of 0.25 V was applied to all contact mode scratching experiments because it was found suitable for removing covalently bonded mono- or multilayer without affecting bare PPF. Moreover, the applied set-point voltage of 0.25 V was suitable for all silicon probes used (RTESP) without prior force calibration.

Figure 1 shows sample AFM images of PPF (right) and PPF modified by reduction of terphenyldiazonium ion (left). For both the TP/PPF surface and unmodified PPF, a 500 nm × 500 nm scratch was made by rastering the tip in contact mode with a set-point voltage value of 0.25 V. The images shown were acquired in tapping mode after "scratching", and line profiles through each scratch are also shown in Figure 1. The image and line profile for the unmodified PPF surface show some debris around the scratch but no discernible damage to the PPF surface. The rms roughness for PPF is <5 Å, as reported previously,[29] and observable defects were quite rare. The flatness and high quality of the PPF surface is presumably due to high-temperature curing in an H_2-containing atmosphere and the lack of any polishing after curing.[29]

Three line profiles drawn at random positions in the TP/PPF scratch are shown in Figure 2. Since the height axis is magnified significantly relative to the *x* and *y* axes, the ridges of debris around the scratch are not as tall as they appear relative to the scratch width. Although all three profiles show a clear trench indicative of the TP layer thickness, there is variation in the apparent trench depth within a given profile and between different profiles. To avoid possible bias by the observer, a statistical procedure was devised to average the trench depth over a large fraction of the scratch area. As shown in Figure 3, a rectangle was defined on the image, which included both scratched and unscratched regions. Lines were defined across this rectangle arbitrarily, one inside the scratch and one outside. The average height along each line was calculated by the AFM software, and then the trench depth was determined by calculating the difference between the mean heights along the lines inside and outside of the scratch. This difference is designated as "line 1" in Table 1 and represents the average layer thickness between the lines shown in Figure 3. "Line 2" was determined in the same fashion after the two lines were increased laterally (to the right in Figure 3) by 100-nm increments. Such increments were repeated through the entire rectangle to generate 5−12 "lines" within each rectangle. The mean and standard deviation of the height difference of these "lines" provide the trench depth and, therefore film thickness, averaged over a large fraction of the rectangle. The "ripple" apparent in the images contributes slightly to the observed rms roughness, but these contributions are largely averaged out by the statistical procedure. Figure 3 shows an averaged depth profile obtained from the TP/PPF image obtained from the average height along each line. This averaged profile is less noisy than those in Figure 2 because each point is an average across the short axis of the rectangle. In some cases, the increment size was larger than 100 nm in order to cover a larger area. For most scratches, a second rectangle was drawn perpendicular to the first, and the same height analysis was performed.

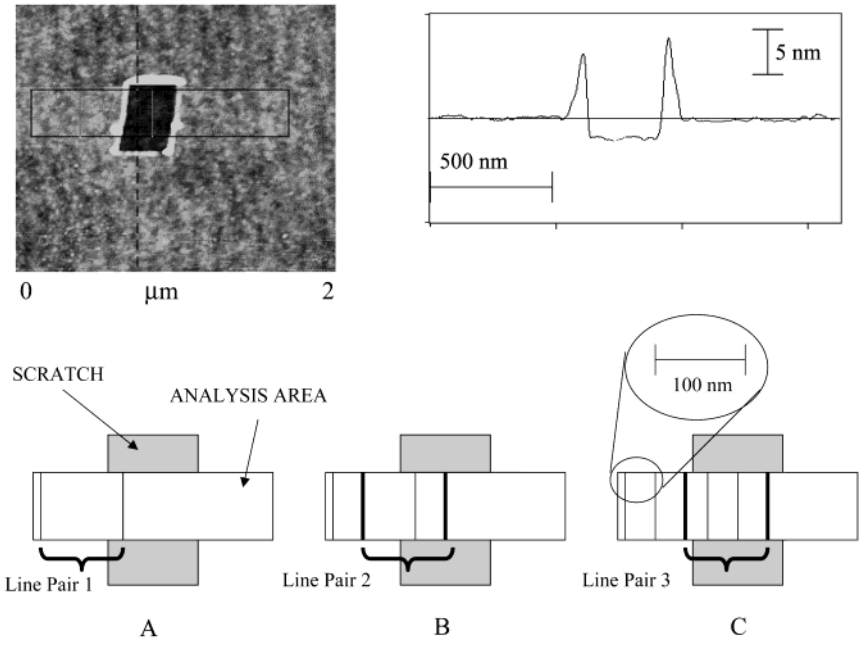

Figure 3. Schematic of statistical method used to determine film thickness. A pair of lines was chosen randomly, one line inside and one outside the scratch. The depth was calculated as the difference in the average height of each line in a pair. Upper right trace shows the profile of the average height through the scratch.

Table 1 compares film thickness variation for three independent samples of PPF derivatized with four voltammetric scans to −0.6 V versus Ag^+/Ag in 1 mM NAB diazonium ion solution (referred to herein as "NAB-4"). Each sample was scratched, and seven to eight "lines" were analyzed for each scratch as previously described. For a given rectangle, the relative standard deviation of the scratch depth varied from 4 to 8%, while the relative standard deviations (RSD) for all 43 lines on three samples was 12%. The average scratch depths for three completely independent samples were 4.40, 4.23, and 5.28 nm, implying some variation in layer thickness for separate NAB derivatizations. Note also that the observed mean scratch depth of 4.28−5.28 nm significantly exceeds that expected for a true monolayer. Based on Gaussian 98[32] calculations and including the van der Waal radius of the terminal oxygen atom, a true NAB monolayer should have a thickness of 1.43 nm, relative to the PPF surface.

The results shown in Figures 1−3 and Table 1 imply that AFM scratching provides a direct and reasonably reproducible indication of modification layer thickness, but they do not provide a calibration of the accuracy of the scratch depth. In fact, the observed layer thickness of ∼4.5 nm for NAB4 is itself surprising, since it corresponds to a film thickness of three or more NAB molecules. To verify the accuracy of the scratch depth, a variety of monolayers was examined, some of which have thicknesses predictable from molecular geometry. Figure 4 shows mean profiles through scratches made using deposition conditions expected to yield true monolayers for PPF modified with stilbene-, biphenyl-, nitrobiphenyl-, and terphenyldiazonium reagents. In each case, one voltammetric cycle between +0.4 and −0.6 V versus Ag^+/Ag and back in 1 mM diazonium ion solution was used for derivatization.

The mean layer thicknesses determined in the same fashion as that illustrated for NAB-4 are listed in Table 2 for all modified PPF surfaces studied. In addition, the rms roughness over relatively large areas was determined and is listed in Table 3. The areas used for determining the rms roughness varied for different modified surfaces but in all cases were larger than the size of both a single molecule and a typical trench. The one-scan films such as nitrobiphenyl (NBP-1) and terphenyl (TP-1) have rms roughness values slightly higher than the PPF substrate. One would expect the rms roughness of an undisturbed monolayer (Table 2) to be comparable to or smaller than the standard deviation of the trench depth (Table 3, third data column). Since trench depth is the difference between the substrate and monolayer heights, the standard deviation of the depth should be ∼1.4 times the rms roughness of substrate or monolayer. The observed standard deviations for trench depth are generally smaller than this estimate (e.g., TP-1 (−0.6 V), possibly because the procedure used to measure trench depth corrects for long-range variation in PPF flatness, and the areas used for Table 3 are larger than those for Table 2.

It is clear from Table 2 that the use of multiple derivatization scans results in greater film thickness, indicating the formation of multilayers. Figure 5 shows a plot of the film thickness resulting from multiple derivatization scans for biphenyl, terphenyl, nitrobiphenyl, and nitroazobenzene. For biphenyl, the observed thickness increases slowly with additional derivatization scans, while the NAB thickness rapidly exceeds the 1.43 nm calculated for a true monolayer. Biphenyl, nitrobiphenyl, and NAB were examined more closely by using less negative derivatization scans to 0.0, −0.2 and −0.4 V versus Ag^+/Ag. Figure 6 shows AFM images of four biphenyl samples scratched after derivatization with scans to 0.0, −0.2, −0.4, and −0.6 V versus Ag^+/Ag. Also shown in Figure 6 and Table 2 are the means and RSDs obtained from the procedure illustrated in Figure 3. The −0.6-V image appears smooth and has the lowest RSD of the four, with a mean thickness a few angstroms larger than that predicted for a true BP monolayer. The images of samples derivatized with less negative

Table 1. Observed Film Thickness (nm) for NAB-4[a] Films

	rectangle 1	rectangle 2
	Sample 1	
line 1	4.114[b]	4.225
line 2	3.982	4.436
line 3	4.136	4.767
line 4	4.268	4.667
line 5	4.321	4.805
line 6	4.619	4.570
line 7	4.399	4.370
line 8	4.351	4.443
mean	4.274	4.535
std dev	0.185	0.202
	Sample 2	
line 1	4.463	3.567
line 2	4.600	3.848
line 3	4.305	4.036
line 4	4.074	3.942
line 5	4.500	4.036
line 6		4.093
line 7		4.411
line 8		4.693
mean	4.388	4.078
std dev	0.205	0.343
	Sample 3	
line 1	4.465	5.724
line 2	5.082	5.851
line 3	5.132	5.732
line 4	4.565	5.579
line 5	4.920	5.686
line 6	4.988	5.835
line 7	4.880	5.621
mean	4.862	5.782
std dev	0.254	0.101
mean for 43 lines on 3 samples	4.64	
std dev	0.58	

[a] Four derivatization scans to −0.6 V vs Ag^+/Ag. [b] Each value is the difference between the average heights of a line pair with each rectangle, one inside and one outside the trench.

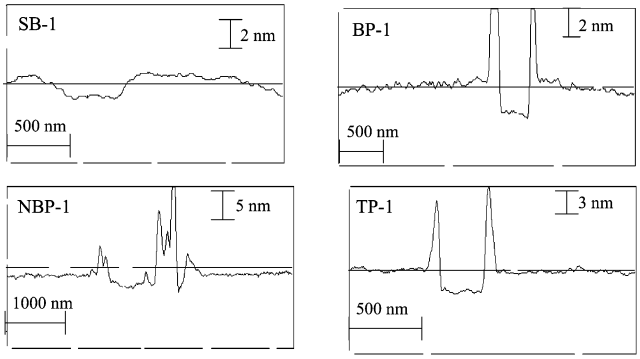

Figure 4. Mean line profiles for stilbene (SB-1), biphenyl (BP-1), nitrobiphenyl (NBP-1), and terphenyl (TP-1) monolayers, each obtained with one derivatization scan to −0.6 V vs Ag^+/Ag.

scans have high RSDs, and apparent "high spots" are observed. These height irregularities are likely to be due to incomplete coverage of the PPF until the −0.6 V negative limit is reached. The situation is different for nitrobiphenyl, as shown in Figure 7 and Table 2. The −0.6-V film has a mean thickness (2.2 nm) almost twice that predicted geometrically (1.21 nm) and shows "spots" similar to those on incompletely derivatized biphenyl. For NBP, the −0.4-V image appears smooth, and less negative potentials yield apparent submonolayer coverage. An obvious possibility for nitrobiphenyl is that multilayer formation starts when the derivatization scan progresses negative of −0.4 V versus Ag^+/Ag, and the "spots" in the −0.6 V image are due to a partial second layer of NBP attached to the initial monolayer.

DISCUSSION

Before considering any quantitative measures of monolayer thickness, it is necessary to consider the most basic issue of whether the model of a "scratched" film as a well-defined rectangular trench is, in fact, accurate. The upper right image of Figure 1 shows no visible damage to bare PPF from the same force used to dig a trench in a modified surface, as expected for the hard, glassy structure of PPF. Furthermore, the statistical procedure described in Table 1 and Figure 3 yielded a "depth" of a scratch in unmodified PPF of 0.37 ± 0.13 nm, much shallower than the scratches in any of the modified surfaces examined. So intentional AFM scratching of unmodified PPF causes little or no observable disruption of the surface, except for the small amount of debris apparent in Figure 1. The possibility that a residue of the monolayer remains in the bottom of the trench after scratching is unlikely, given the apparent flatness of the trench bottom. None of the scratches had significant observable deposits of debris inside the scratch, and in all cases, the observed debris at the scratch edges are much thicker than any height variations inside the scratch. In addition, the cantilever forces applied here have been shown to be sufficient to completely remove a 5-nm oxide layer on an aluminum alloy that has been submerged in water.[26,27]

The statistical method for determining average scratch depth was devised to objectively average surface roughness and instrumental noise but also to correct for long-range (>100-nm) variation in PPF flatness or tilt. By averaging the difference between two members of a line pair (as shown in Figure 3), a gradual slope of the PPF or monolayer height is ignored. In effect, the approach corrects for sample tilt and height variations over a lateral distance that is large compared to the scratch dimensions. In addition, the method prevents biasing the results by user choice of particular spots on the monolayer surface or inside the scratch. Since many points are averaged on each of several pairs of lines, an average that objectively represents the sample depth is obtained.

With the exception of stilbene (SB-1), the observed monolayer thicknesses shown in Figure 3 and listed in Table 2 for stilbene, biphenyl, terphenyl, and nitrobiphenyl are slightly higher than the thicknesses calculated from Gaussian 98. This deviation may be due to a layer of adsorbed water or hydrocarbon or to sporadic addition of a second derivatization layer. Even if this apparent overestimate of thickness were considered a systematic error, the method would still be adequate for detecting widespread multilayer formation. For example, the continued growth of a nitroazobenzene film with additional derivatization scans (Figure 5) clearly demonstrates multilayer formation, since the thickness increases monotonically to 6.3 nm for 10 derivatization scans. This result indicates an NAB film that is much thicker than calculated for a monolayer of NAB molecules, whether or not a ∼35% error is present. The single-scan cases in Table 1 (SB-1, BP-1, NBP-1, NAB-1, TP-1) used derivatization conditions normally employed for monolayer formation, and the AFM results confirm that true monolayers are formed for at least stilbene and biphenyl. However,

Table 2. Observed Thickness for Films Formed by Diazonium Reduction

	calcd, nm[a]	AFM, mean, nm	AFM std dev, nm	% std dev	no. of samples[b] examined	no. of scratches	no. of rectangles	total no. of lines
bare PPF[c]		0.375	0.155	41	2	2	2	12
SB-1[d] (−0.6 V)[e]	1.34	1.336	0.162	12.1	1	1	2	8
BP-1 (−0.0 V)		0.738	0.318	43.1	1	1	1	25
BP-1 (−0.2 V)		0.932	0.164	17.6	1	1	1	28
BP-1 (−0.4 V)		0.968	0.329	34.0	1	1	1	22
BP-1 (−0.6 V)	1.11	1.507	0.236	15.7	2	2	3	23
BP-4 (−0.6 V)		1.712	0.152	8.9	1	2	3	24
BP-10 (−0.6 V)		2.325	0.956	41.1	1	2	2	14
TP-1 (−0.6 V)	1.523	1.809	0.154	8.5	1	1	2	18
TP-4 (−0.6 V)		2.123	0.153	7.2	1	2	2	28
TP-10 (−0.6 V)		4.416	0.734	16.6	1	2	3	27
NBP-1 (0.0 V)		0.271	0.150	55.3	1	1	1	13
NBP-1 (−0.2 V)		0.644	0.333	51.8	1	2	1	33
NBP-1 (−0.4 V)		1.708	0.210	12.3	1	1	1	14
NBP-1 (−0.6 V)	1.208	2.118	0.504	23.7	3	3	3	18
NBP-4 (−0.6 V)		2.526	0.531	21.0	1	2	4	31
NBP-10 (−0.6 V)		4.229	0.219	5.2	1	1	3	19
NAB-1 (0.0 V)		0.998	0.227	22.8	2	2	4	23
NAB-1 (−0.2 V)		1.884	0.143	7.6	1	1	2	10
NAB-1 (−0.3 V)		2.065	0.163	7.9	1	1	2	12
NAB-1 (−0.4 V)		2.334	0.093	4.0	1	1	1	10
NAB-1 (−0.6 V)	1.43	2.623	0.293	11.2	3	2	6	37
NAB-2 (−0.6 V)		3.245	0.347	10.7	1	2	4	26
NAB-4 (−0.6 V)		4.508	0.682	12.5	3	3	3	43
NAB-10 (−0.6 V)		6.357	0.508	8.0	1	2	4	32

[a] From Gaussian 98, B3LYP/6-31G(d), plus van der Waals radius of terminal atom. [b] "Samples" refers to independently prepared PPF surfaces and monolayers. [c] Control sample, prepared and scratched the same way as monolayer samples. [d] Number indicates number of derivatization scans. [e] Negative potential limit for derivatization scan, stated vs Ag^+ (0.01 M)/Ag.

Table 3. Roughness of Bare and Modified PPF

	area, $\mu m \times \mu m$	rms roughness, nm		
		sample 1	sample 2	average
PPF alone[a]	3.9 × 2.3	0.643	0.409	0.526
SB-1	1.4 × 0.8	0.465	0.461	0.463
BP-1	0.8 × 0.6	0.818		0.818
BP-4	4.0 × 4.0	0.710	0.907	0.809
BP-10	3.6 × 4.1	0.732	0.745	0.739
TP-1	1.2 × 1.0	0.683	0.239	0.461
TP-10	3.3 × 2.8	1.020	0.668	0.844
NBP-1	2.8 × 3.5	0.509	0.597	0.553
NBP-10	2.1 × 1.6	0.810	0.830	0.820
NAB-1	4.0 × 4.0	1.081	0.443	0.762
NAB-2	3.2 × 1.4	0.518	0.497	0.508
NAB-4	0.7 × 0.8	0.365	0.389	0.377
NAB-10	3.8 × 3.9	0.551		0.551

[a] Unmodified PPF carried through all cleaning and processing steps, except for reduction in diazonium ion solution.

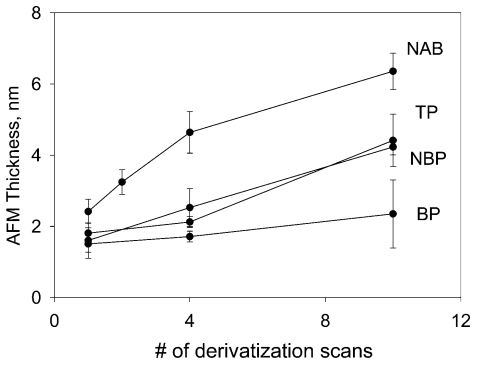

Figure 5. AFM film thickness versus number of derivatization scans to −0.6 V vs Ag^+/Ag. Error bars indicate ± one standard deviation unit of the layer thickness.

there is a clear danger that higher diazonium ion concentrations or more extensive electrolysis during derivatization can lead to unintended multilayers.

Figure 5 and Table 2 show that multilayers are formed for at least NAB, NBP, and TP and more slowly for biphenyl. Since monolayers are often considered "blocking" toward electron transfer, an obvious question arises of how multilayers can form. To reduce diazonium ions in solution after the first monolayer is deposited, electrons must be transported from the PPF substrate through the monolayer. Tunneling may be effective over distances of ~2.0 nm or less, but tunneling should be very slow over larger distances. How can a diazonium reagent be reduced to its reactive radical form through organic films with >4.0-nm thickness? A likely explanation is "conductance switching" reported for biphenyl, NBP, and NAB monolayers, in which electron injection into the monolayer results in a partially conductive film.[19,31] For the case of NAB, this electron injection was monitored spectroscopically,[8] and we proposed that the resulting NAB layer had a significantly lower barrier for electron tunneling.[19,31] Loosely speaking, the organic layer was switched "ON" electrochemically to a more conductive state, permitting relatively fast electron transfer to species in solution.

If such a switching mechanism were operative during derivatization of the PPF surface, it is possible that an initial monolayer of NAB, BP, etc., could become sufficiently conductive to reduce further diazonium ions in solution. The resulting radical could then attack the existing monolayer to form a multilayer. Similar monolayers have been shown to support outer-sphere electron transfer to solution redox couples following negative potential excursions,[31] and even a slow electron transfer through a growing

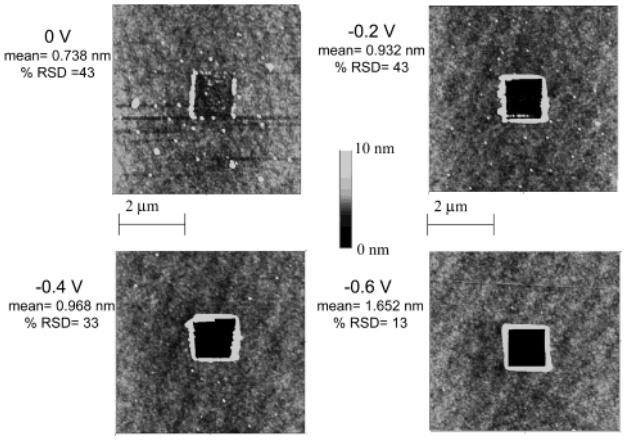

Figure 6. Tapping mode images for a biphenyl-modified PPF surface following a contact mode scratch. Single derivatization scans from +0.4 to 0, −0.2, −0.4, and −0.6 V vs Ag/Ag^+ were used to modify the PPF surface, as indicated. Also shown are the mean thickness and relative standard deviation determined statistically as described in the text.

film would be sufficient to continue film growth. Since this mechanism should be able to continue beyond a second layer, the NAB film grew to at least 6.3 nm, and NBP to 4.2 nm with repeated derivatization scans. Furthermore, Kariuki and McDermott observed multilayers with >20-nm thickness during reduction of diethylaminophenyldiazonium ion,[5] a result that is very difficult to explain by simple tunneling. For the reagents studied here, the order of reduction potential for the parent molecules is NAB > NBP > TP > BP, meaning that free nitroazobenzene reduces at a more positive potential than nitrobiphenyl, etc. The correlation between the ease of reduction and the film thickness listed in Table 2 is consistent with a model based on multilayer formation through conductance switching of the initial monolayer.

Figures 6 and 7 show that deposition potential for even a single derivatization scan affects the resulting layer thickness. A concern arises of whether a true monolayer can form at all, in which coverage is complete, but initiation of a second layer has not occurred. The images of Figures 6 and 7 indicate that smooth monolayers of biphenyl and nitrobiphenyl are indeed formed for single scans to −0.6- and −0.4-V scans, respectively, for the conditions employed (1 mM diazonium reagent, 200 mV/s scan rate). In addition, there are mechanistic grounds to expect a true monolayer to form before the initiation of a second layer. The initial reduction of diazonium reagent occurs at a bare PPF surface, and the maximum density of attachment sites is present. For the second modification layer to form, an electron must transfer through 1−1.5 nm of organic monolayer, and an electrogenerated radical must react with a phenyl ring, presumably involving H atom abstraction or attack of an aromatic double bond. We expect electron transfer to be significantly slower through >10 Å of monolayer, and the reaction of the radical with a phenyl ring should be no faster than that with the PPF surface. Unless electron transfer through the initial monolayer is unexpectedly fast, or the PPF layer is much less reactive than expected, there should be a window during derivatization in which a low-defect true monolayer is formed.

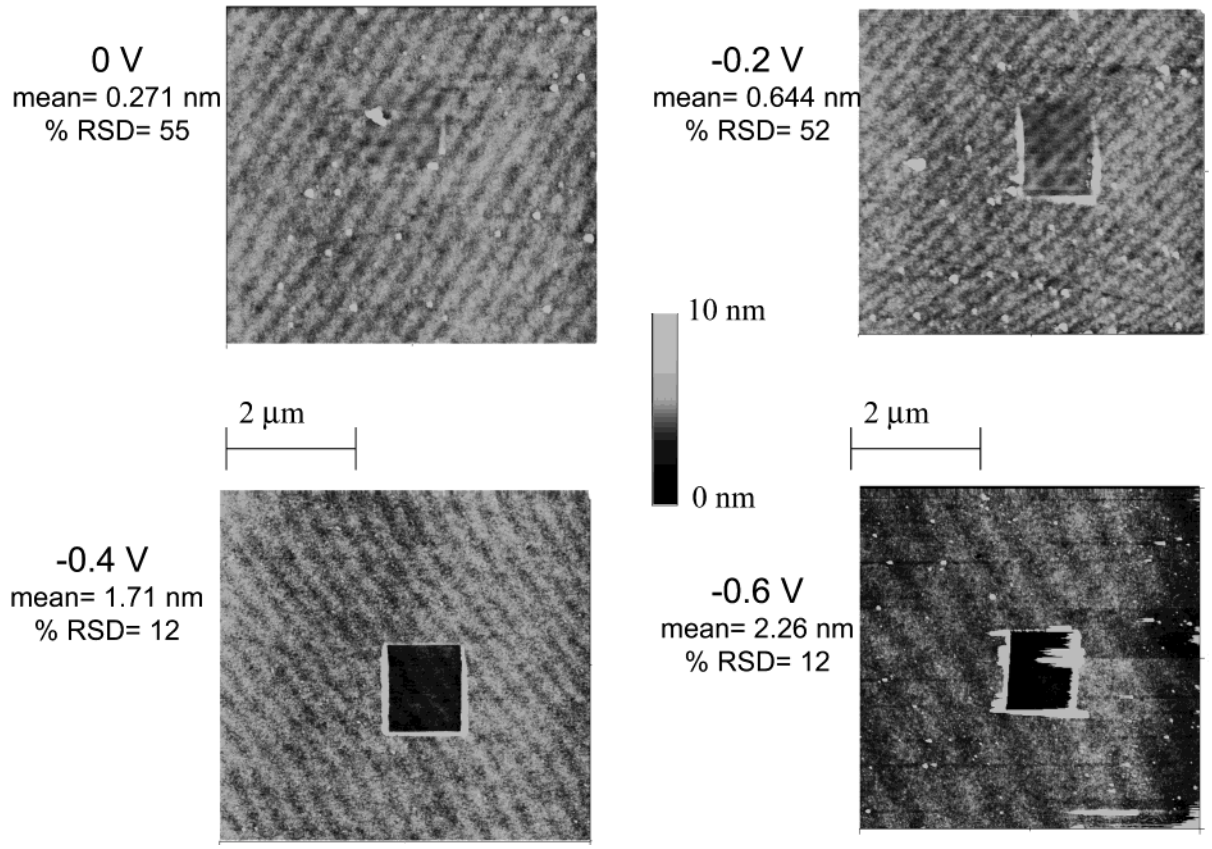

Figure 7. Tapping mode images for a nitrobiphenyl modified PPF surface following a contact mode scratch. Single derivatization scans from +0.4 to 0, −0.2, −0.4, and −0.6 V vs Ag^+/Ag were used to modify the PPF surface, as indicated. Also shown are the mean thickness and relative standard deviation determined statistically as described in the text.

That said, it is clear that derivatization conditions are critical to producing a monolayer without progressing to multilayer films. The low reagent concentrations ($\leq$1 mM) and relatively short electrolysis times used by many investigators are generally suitable for monolayer formation on glassy carbon. However, Kariuki and McDermott noted that high diazonium concentrations or extensive electrolysis can result in thick multilayers,[5] and the results reported here demonstrate formation of multilayers of NBP and NAB with supposedly gentle conditions. The AFM scratching experiment described here is an objective measure of layer thickness that does not require any assumptions about electron transfer through a monolayer. Wherever possible, we strongly recommend verification of monolayer formation when testing new reagents or conditions. We plan to continue to use AFM to evaluate layer thickness for monolayers on PPF and the activity of a modified surface toward dopamine oxidation as a test for pinholes.[13,31]

Finally, the formation of monolayers by diazonium ion reduction can be compared to the widely studied thiol adsorption to metal surfaces to yield self-assembled monolayers (SAMs).[33,34] Since SAM formation requires a metal−thiol bond, covalent multilayers are not possible unless the thiol reagent is specifically designed to form additional layers. SAM formation is an equilibrium process, with desorption and readsorption resulting in annealing of the SAM to produce an ordered monolayer. The bonding of a radical produced by diazonium reduction is irreversible, and annealing is unlikely. However, pinholes in an incomplete monolayer facilitate electron transfer to diazonium reagent, thus patching the pinhole. Provided the initial reduction and radical attack to the carbon surface are significantly faster than formation of the second layer, an irreversibly attached, low-pinhole monolayer results. The aggressive, irreversible binding of radicals electrogenerated from diazonium reagents yields a robust monolayer that is prone to multilayer formation, but monolayer formation is achievable with the aid of a direct measure of layer thickness to define derivatization conditions.

(33) Finklea, H. O. Electrochemistry of Organized Monolayers of Thiols and Related Molecules on Electrodes. In *Electroanalytical Chemistry*; Bard, A. J., Ed.; Dekker: New York, 1996; Vol. 19; p 109.
(34) Porter, M. D.; Bright, T. B.; Allara, D. L.; Chidsey, C. E. D. *J. Am. Chem. Soc.* **1987**, *109*, 3559.

ACKNOWLEDGMENT

This work was supported by the Analytical and Surface Chemistry Division of the National Science Foundation and by ZettaCore, Inc. Useful conversations with Prof. Gerald Frankel and Dr. Patrick Leblanc were appreciated, as was use of an AFM purchased with AFOSR funds. The authors also acknowledge reviewers' comments pointing out precedents for the AFM scratching technique.

Received for review January 10, 2003. Accepted May 5, 2003.

AC034026V